scientific reports

Check for updates

OPEN

Magnetic nickel nanoparticle catalyst on β-cyclodextrin-modified Fe_3O_4 for nitroarene hydrogenation

Sara Payamifar[1], Amin Foroozandeh[1], Majid Abdouss[1] & Ahmad Poursattar Marjani[2]✉

This study developed a novel and highly active heterogeneous catalyst of nickel nanoparticles supported on β-cyclodextrin-grafted magnetic Fe_3O_4 nanoparticles (Ni@β-CD@Fe_3O_4). β-CD, a biodegradable, biocompatible, green, and non-toxic cyclic oligosaccharide, was modified with Fe_3O_4 nanoparticles to create β-CD@Fe_3O_4. The nickel was then immobilized onto this support. The catalyst was characterized using FT-IR, XRD, TEM, AAS, FE-SEM, TGA, EDX, DRS-UV-Vis spectra, and VSM techniques. The catalytic activity of Ni@β-CD@Fe_3O_4 was evaluated for the reduction of nitroarene compounds in water at 25 ℃. This nanocatalyst indicated great activity and selectivity in reducing various nitroarenes, including nitrobenzene, nitroaniline, nitrotoluene, and nitrophenol derivatives. Additionally, the catalyst showed significant reusability and could be easily separated using an external magnet, highlighting its potential for green chemistry and sustainable industrial applications.

Keywords Reduction, Nitroaromatic compound, β-Cyclodextrin (β-CD), Nickel, Amine

Pursuing sustainable and environmentally friendly methods in chemical synthesis is pivotal in contemporary organic chemistry. The imperative to minimize chemical waste and reduce organic pollutants underscores the principles of green chemistry[1–3]. Nitroaromatic compounds, known for their toxicity and environmental hazards, represent a significant challenge. In contrast, their reduction to amino derivatives is essential in various industrial sectors, including pharmaceuticals and agrochemicals[4–7].

The progress of efficient and sustainable catalysts for reducing nitroarenes has recently garnered considerable attention[8–10]. Although effective, traditional methods, such as the Béchamp reduction using iron or ferrous salts, suffer from drawbacks, including the generation of substantial chemical waste and reliance on mineral acids[11]. In contrast, catalytic hydrogenation using transition metals has emerged as a promising alternative[12–15].

Palladium catalysts have been extensively studied and utilized to reduce nitroaromatics due to their high activity. However, their widespread application is hindered by the overpriced and poisonous associated with Pd and its derivatives[16–20]. In response, there is a growing interest in exploring cost-effective and less toxic alternatives, such as nickel-based catalysts, which offer comparable reactivity and are more abundant[21–26].

Recently, drastic notice has been given to using magnetite nanoparticles (Fe_3O_4) as excellent recyclable support for transition metals, such as palladium[27], copper[28], and nickel[29]. The high chemical stability, large surface area, simple separation by an external permanent magnet and recovery, non-toxicity, readily accessible, low cost, and environmental compatibility are some prominent advantages of magnetic nanoparticle catalysts. Also, the heterogeneous catalysts particularly supported catalysts, have been given significant attention lately[30–33].

Among the various supramolecular catalysts, β-cyclodextrins (β-CDs) have gained prominence due to their environmentally benign nature and unique molecular structure. β-CDs are cyclic oligosaccharides derived from the enzymatic conversion of starch, characterized by a hydrophobic central hollow and a hydrophilic exterior cover. β-CDs can create inclusion complexes with a wide range of guest molecules without forming covalent bonds, thereby serving as versatile and biocompatible materials[34–38]. The use of β-CDs in catalysis has been widely explored across different fields, highlighting their potential in sustainable chemical transformations[39–47].

Reducing nitroaromatic compounds to less toxic amines using β-CD-based catalysts represents a significant advancement in green chemistry[9,10,48–51]. Recently, Hasan et al. reported the synthesis of a heterogeneous catalyst, Fe_3O_4@β-CD@Pd, demonstrating promising catalytic activity for nitroarene reduction under mild conditions[52]. Inspired by these advances, our study focuses on developing and identifying a new catalyst system based on nickel nanoparticles supported on β-CD grafted magnetic nanoparticles of Fe_3O_4 (Ni@β-CD@Fe_3O_4).

This research addresses current limitations associated with existing catalysts, such as high cost and toxicity. As a transition metal, nickel offers a cost-effective and environmentally benign alternative to palladium, while

[1]Department of Chemistry, Amirkabir University of Technology, Tehran, Iran. [2]Department of Organic Chemistry, Faculty of Chemistry, Urmia University, Urmia, Iran. ✉email: a.poursattar@urmia.ac.ir; a.poursattar@gmail.com

β-CDs provide a robust and eco-friendly support matrix. Our catalyst aims to combine the high reactivity of nickel with the advantageous properties of β-CDs and magnetic nanoparticles (Fe_3O_4), enabling efficient catalytic conversion of nitroarenes into their corresponding amines under aqueous conditions.

The importance of current work depends on its potential contributions to sustainable chemistry, where reducing toxic nitroaromatic pollutants using a recyclable and efficient catalyst system aligns with the principles of green chemistry. By leveraging the synergistic effects of nickel nanoparticles and β-CDs grafted onto magnetic nanoparticles, we anticipate achieving high catalytic activity, selectivity, and recyclability, paving the way for practical applications in pharmaceutical and fine chemical industries.

This introduction outlines the critical importance of developing green and sustainable catalytic systems for organic transformations. It provides a rationale for exploring novel catalysts based on nickel nanoparticles supported on β-CD grafted magnetic nanoparticles of Fe_3O_4 to reduce nitroarenes, highlighting the potential benefits over existing methodologies. The subsequent sections will detail the experimental methods, characterization techniques, and results obtained, culminating in a comprehensive evaluation of the catalytic performance and prospects for future research directions.

Results and discussion

β-CD, as a green renewable cyclic oligosaccharide and inexpensive chemically stable available material, has excellent potential to be used as a support and ligand to stabilize metal nanoparticles. In this regard, our recent review explained the advances in β-CD-based catalysts for reducing toxic nitroaromatic[10]. This paper shows further significant applications of the β-CD-supported nickel nanoparticles for reducing toxic nitroaromatic using low nickel loading at 70 °C in water.

The stepwise synthesis pathway of the catalyst is shown in Fig. 1. Fe_3O_4 nanoparticles were made ready based on the strategy of Massart employing $FeCl_3{\cdot}6H_2O$ and $FeCl_2{\cdot}4H_2O$[53]. The β-CD was sonicated with magnetic nanoparticles at 70 °C overnight to produce β-CD@Fe_3O_4 NPs. The Ni@β-CD@Fe_3O_4 was gained quickly by dissolving $Ni(OAc)_2$ in distilled water and adding β-CD@Fe_3O_4, also dissolved in H_2O by sonication, at 70 °C for one day.

Characterization

FT-IR analysis

The obtained Ni@β-CD@Fe_3O_4 nanoparticles were identified utilizing the FT-IR technique, which is displayed in Fig. 2. The spectrum of β-CD indicated the absorption bands at $\nu = 3000–3900\ cm^{-1}$ that belong to the stretching vibrations of the hydroxyl group and peak at $\nu = 1157\ cm^{-1}$ relevant to asymmetric glycosidic C–O–C vibration.

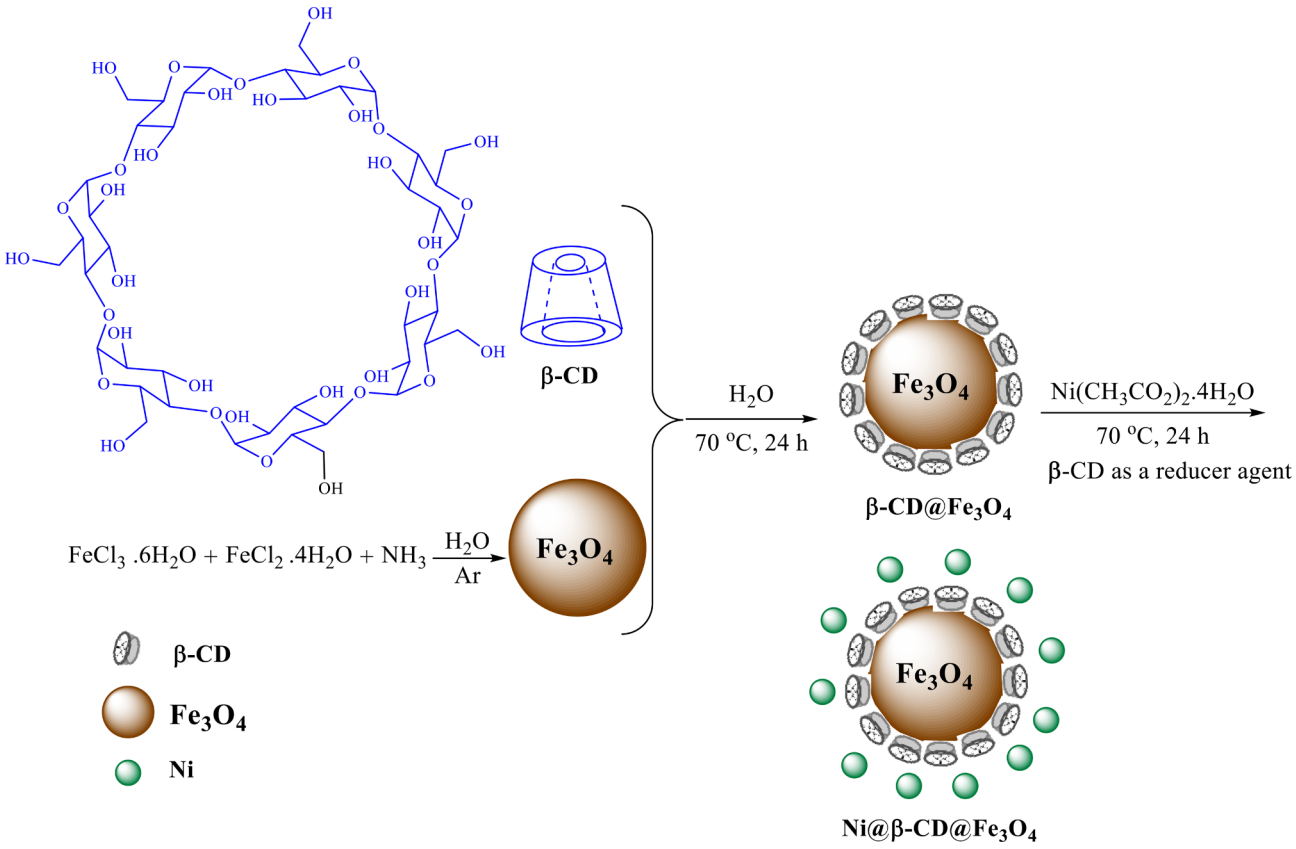

Fig. 1. Preparation steps of Ni@β-CD@Fe_3O_4 NPs.

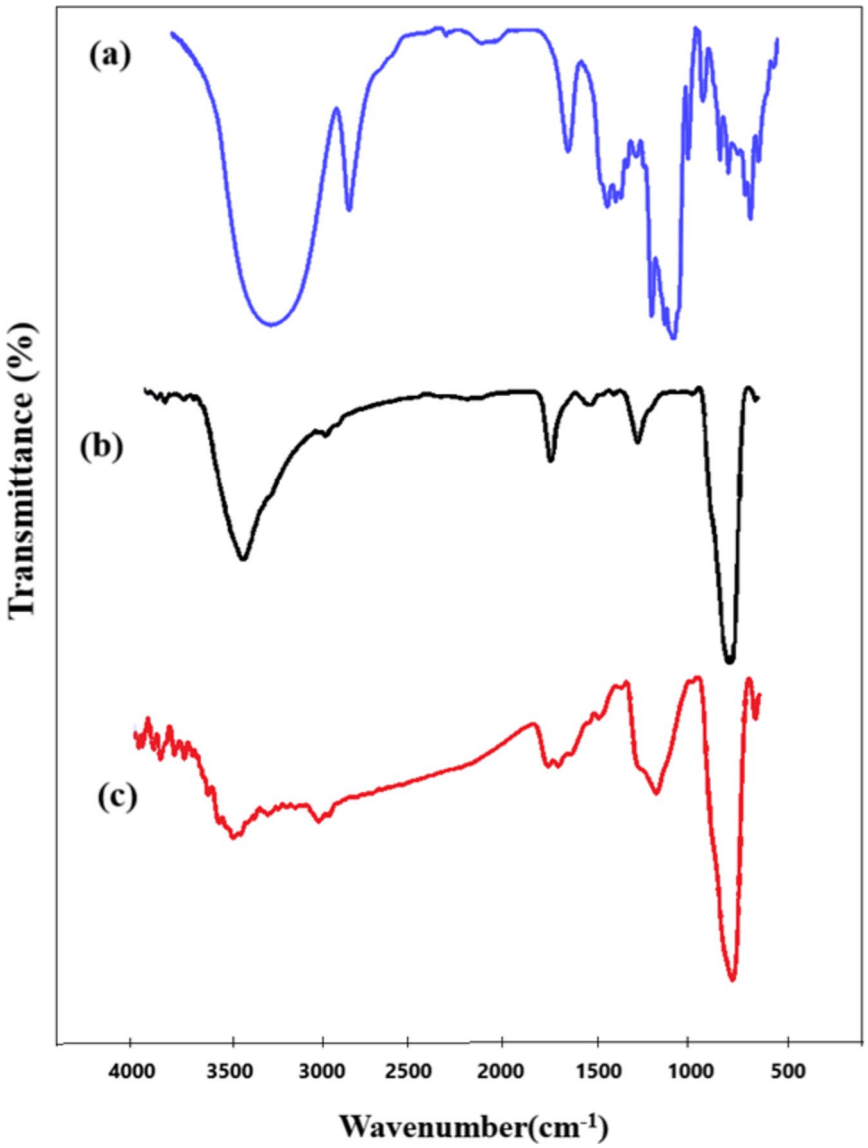

Fig. 2. FT-IR spectra of β-CD (**a**), Fe_3O_4 (**b**), and Ni@β-CD@Fe_3O_4 (**c**).

The band at 570 cm^{-1} corresponds to O–Fe stretch and strong band absorption at 3400 cm^{-1} in accordance with –OH stretching vibration for magnetic nanoparticle bonding. For Ni@β-CD@Fe_3O_4, spectra were found to be narrowed in the FT-IR spectrum after being bonded with $Ni(OAC)_2$ which is suitable proof of the formation of the inclusion complex and did not display a carbonyl group absorption band, which verifies that the acetate anion has been deleted after the process of reduction of Ni(II) to Ni(0). Here, we didn't use a reducer agent. Based on our previous works with β-CD and nickel, β-CD acts as a reducer agent and reduces Ni(II) to Ni(0). Ni(0) species is generated in the presence of β-CD. We assume that the role of β-CD is to stabilize the active catalyst[44,45]. The FT-IR results prove that magnetite nanoparticle functionalization has been done successfully.

FE-SEM and TEM analysis

The FE-SEM image of the Ni@β-CD@Fe_3O_4 indicated the construction of mono-dispersed and uniform spherical particles (Fig. 3a–c). The TEM image in Fig. 3d indicates that the Ni@β-CD@Fe_3O_4 NPs are almost spherical with an average size of approximately 10–20 nanometers. The boundary between the particles (low contrast) was not detectable in the TEM of the Ni@β-CD@Fe_3O_4, which may be due to interactions between the neighboring particles. No significant layer of Ni@β-CD could be observed on these nanoparticles[54].

EDX analysis

The energy-dispersive spectrum (EDX) obtained from FE-SEM analysis proved the presence of diverse elements in the material's structure, like Ni, Fe, O, and C species (Fig. 4). Quantitative results of EDX data are shown in Table 1.

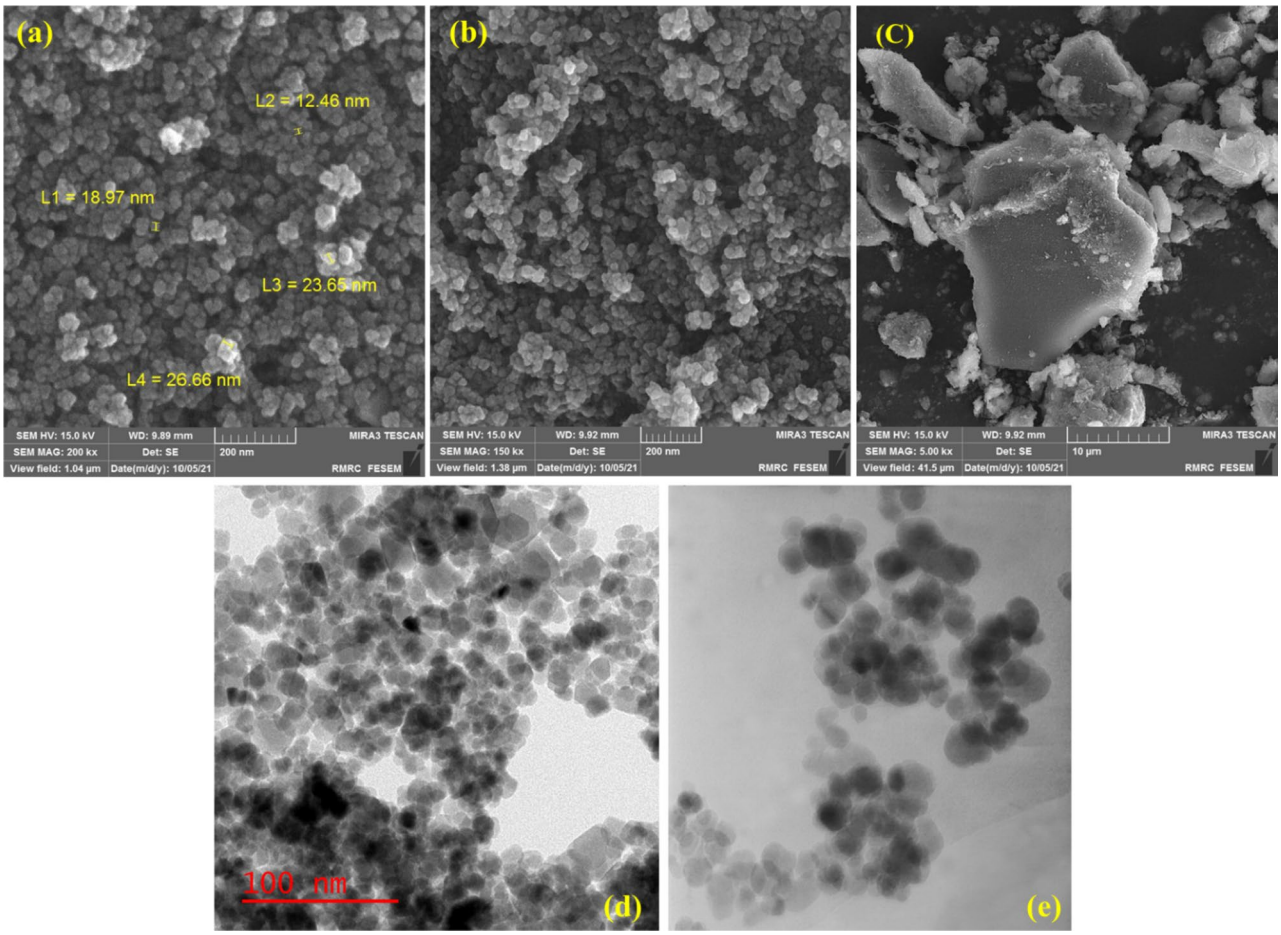

Fig. 3. FE-SEM images of Ni@β-CD@Fe_3O_4 in different magnifications (**a–c**), TEM of Ni@β-CD@Fe_3O_4 (**d**), and Fe_3O_4 (**e**).

XRD analysis

Powder X-ray diffraction (XRD) study of Ni@β-CD@Fe_3O_4 displayed peaks at 2θ values 2θ = 30.3°, 35.7°, 37.3°, 43.3°, 53.8°, 57.4°, and 63.0° are relevant to (220), (311), (222), (400), (511), and (400) planes of $NiFe_2O_4$ structure (JCPDS card no. 54–0964). (Fig. 5)

VSM analysis

The magnetic features of this nanocatalyst were analyzed with a VSM. The superparamagnetic character of Ni@β-CD@Fe_3O_4, Fe_3O_4 NPs, and reused catalysts was also investigated. The observed results demonstrated that a decline in the magnetization value of the Ni@β-CD@Fe_3O_4 (50 $emug^{-1}$) in comparison with that of Fe_3O_4 NPs (64 $emug^{-1}$), which shows the magnetic property of Fe_3O_4 is reduced by coating and approves the modification of Fe_3O_4 NPs (Fig. 6). However, the Ms. Value of Ni@β-CD@Fe_3O_4 was sufficiently high, which can still be separated quickly from the solution using a magnet bar.

TGA analysis

The TGA curve of Ni@β-CD@Fe_3O_4 nanoparticles (NPs) provides valuable insights into the composite material's thermal stability and decomposition patterns (Fig. 7). The TGA profile reveals several distinct weight-loss stages corresponding to different thermal events within the sample.

Stage 1: Weight Loss Below 150 °C.

The initial weight loss of 1.37% observed below 150 °C is attributed to the evaporation of the sample's physically adsorbed solvents and water molecules. This low-temperature weight loss is typical for many nanoparticle systems where residual solvents and moisture are present on the surface or within the material's pores.

Stage 2: Weight Loss from 200 to 400 °C.

In the temperature range of 200 to 400 °C, a more significant weight loss of 4.17% is observed. This stage indicates the decomposition of organic components within the Ni@β-CD@Fe_3O_4 NPs. The β-CD component, an organic molecule, decomposes in this temperature range. The observed weight loss can be correlated with the thermal degradation of β-CD as it breaks down into more minor volatile compounds.

Stage 3: Weight Loss from 400 to 550 °C.

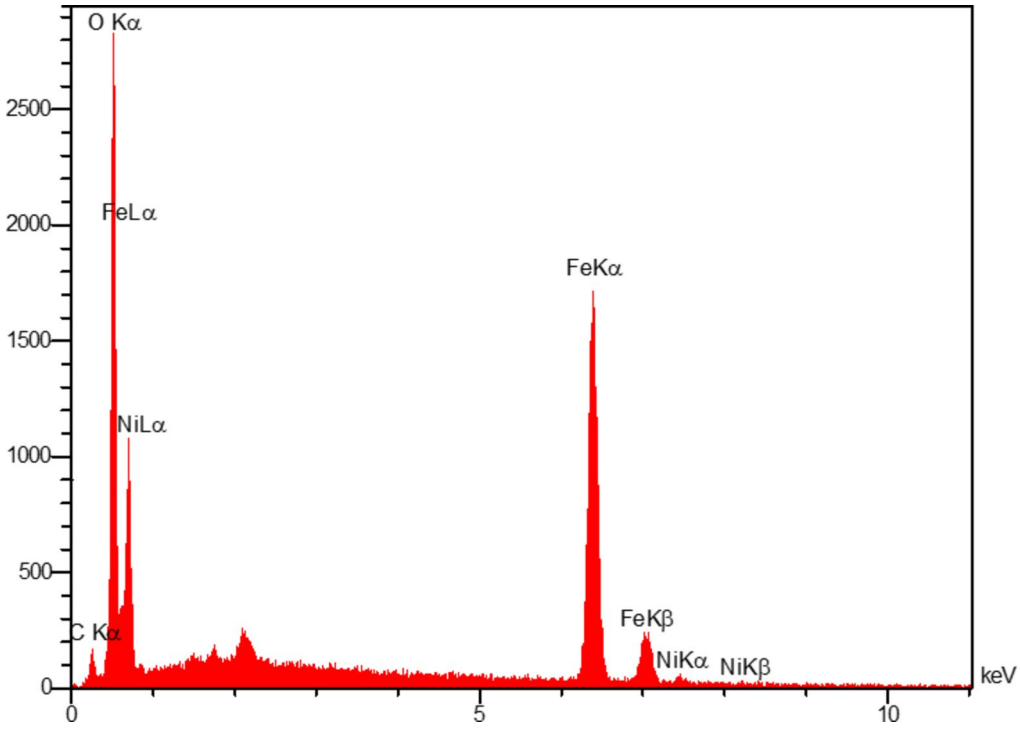

Fig. 4. EDX spectrum of Ni@β-CD@Fe_3O_4.

Nanomagnetic catalyst	The weight% of iron	The weight% of carbon	The weight% of oxygen	The weight% of nickel
Ni@β-CD@Fe_3O_4	53.21	8.10	37.04	1.65

Table 1. Quantitative results of EDX data.

As the temperature increases from 400 to 550 °C, a second notable weight loss of 3.61% is recorded. This weight loss is predominantly associated with the further decomposition of β-CD and any remaining organic residues. The β-CD undergoes complete thermal degradation at these elevated temperatures, resulting in additional weight loss.

The TGA curve of Ni@β-CD@Fe_3O_4 NPs indicates a total weight loss of approximately 9.15% up to 550 °C. This weight loss is primarily owing to the decomposition of the β-CD component and the desorption of physically adsorbed solvents and water. The TGA data confirm the presence of β-CD in the composite material and estimate its thermal stability. The observed thermal degradation pattern is consistent with the expected behavior of β-CD-based nanocomposites, where initial weight loss corresponds to desorption of adsorbed species followed by decomposition of the organic matrix.

These thermal properties are essential for understanding the stability and potential applications of the Ni@β-CD@Fe_3O_4 NPs, especially in processes that involve elevated temperatures. The material's thermal stability ensures its suitability for catalytic applications, where temperature resilience is often required.

To study the performance of the prepared Ni@β-CD@Fe_3O_4 NPs as a nanocatalyst for the nitro reduction reactions, the hydrogenation of 4-nitrotoluene was selected as a pattern reaction, and the influence of different items like solvent, reducing agent, and quantity of catalyst were studied (Table 2). Various solvents were listed, and the results indicated that the amine product was provided with down-to-average yields (Table 2, entries 1–11). The influence of some reducing agents was also checked, and the results indicated that the role of sodium borohydride is crucial for this reaction (Table 2, entries 13–16). Reducing the quantity of nickel NPs to 1 mol% induced a notable drop in yields (Table 2, entry 17).

To investigate the catalytic performance of the synthesized Ni@β-CD@Fe_3O_4 NPs in nitro reduction reactions, we selected the reduction of 4-nitrotoluene as a pattern reaction. We evaluated the effects of diverse parameters on the reaction efficiency, including solvent, the reducing agent, and catalyst quantity (Table 2).

Optimization of reaction conditions

Nickel loading on the Ni(II)-β-CD complexes was 1.37 ppm, measured by atomic absorption spectroscopy (AAS). We began by screening different solvents for reducing 4-nitrotoluene using Ni@β-CD@Fe_3O_4 NPs (15 mg, 1.5 mol% of Ni) and $NaBH_4$ (0.8 mmol) at 25 ℃. The solvents tested included DMF, THF, toluene, DMSO, dichloromethane, 1,4-dioxane, ethyl acetate, PEG200, ethanol, acetone, methanol, and water. The yields of the reduction product varied significantly, with water proving to be the most effective solvent, providing a

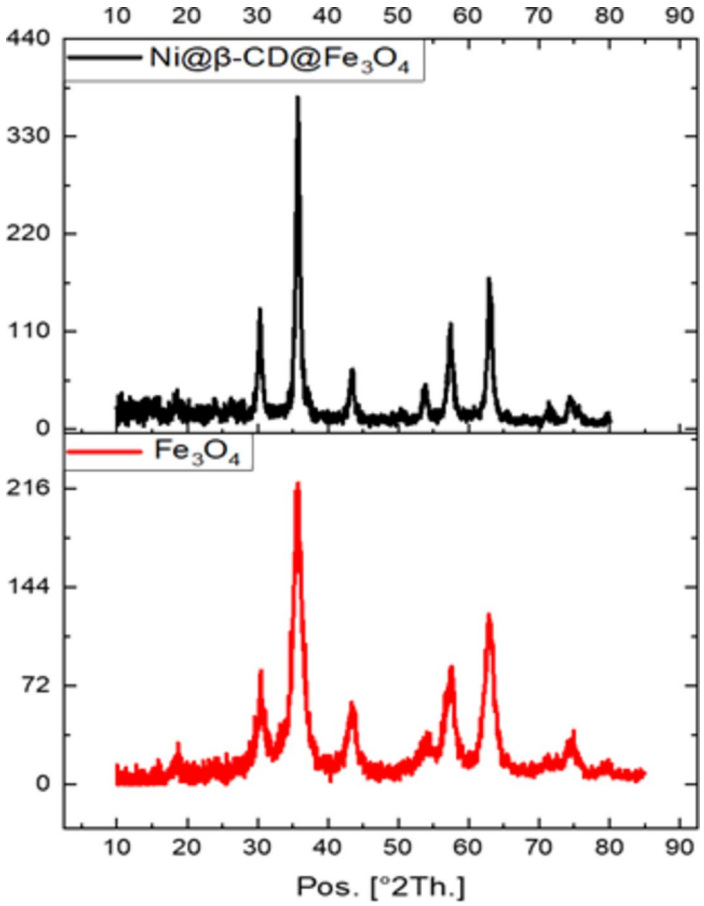

Fig. 5. XRD pattern Fe_3O_4 and Ni@β-CD@Fe_3O_4 NPs.

100% yield (Table 2, entry 12). Other solvents yielded lower efficiencies, with ethanol (71%), acetone (65%), and methanol (35%) following (Table 2, entries 9, 10, and 11).

Next, we explored the influence of different reducing agents on the reaction in water. The reducing agents tested were isopropyl alcohol, ammonium formate, glycerol, and hydrazine. $NaBH_4$ was found to be essential for the reaction, with other agents resulting in no reaction or significantly lower yields (Table 2, entries 13–16).

We also examined the effect of reducing the catalyst quantity. Lowering the catalyst loading to 1 mol% led to a notable drop in yield to 42%, demonstrating the importance of using an adequate amount of catalyst for optimal performance (Table 2, entry 17).

By having the optimized conditions, the reduction of a variety of nitroaromatic compounds was evaluated (Table 3). Results demonstrated that the hydrogenation of nitroarenes carrying electron-withdrawing groups like –F, –Br, –Cl, and –I performed successfully, and expected products were provided in high yields. The hydrogenation of nitroarenes containing electron-donating groups like –OH, –Me, –OMe, $–CH_2OH$, and $–NH_2$ was conducted, and the desired amines were afforded in good to superb yields (Table 3, entries 1–20).

Evaluation of catalytic performance

With the optimized reaction conditions established (water as the solvent, $NaBH_4$ as the reducing agent, and 1.5 mol% catalyst loading), we proceeded to evaluate the catalytic performance of Ni@β-CD@Fe_3O_4 NPs for the reduction of diverse nitroaromatic compounds (Table 3).

Nitroarenes having electron-withdrawing groups (e.g., –F, –Br, –Cl, and –I) were efficiently reduced to their corresponding amines in high yields, showcasing the catalyst's effectiveness (Table 3, entries 1–8). Similarly, nitroarenes with electron-donating groups (e.g., $–NH_2$, $–CH_2OH$, –OMe, and –Me) were also reduced effectively, yielding the desired amines in good to high yields (Table 3, entries 9–20).

Comparison of catalytic activity

A comparison of the results of the present system with the previous reports is shown in Table 4.

Catalyst recycling

The hydrogenation of 4-nitrotoluene under the optimal reaction conditions was examined to evaluate the recoverability power of this nanocatalyst. For this purpose, in each cycle, the aqueous medium containing

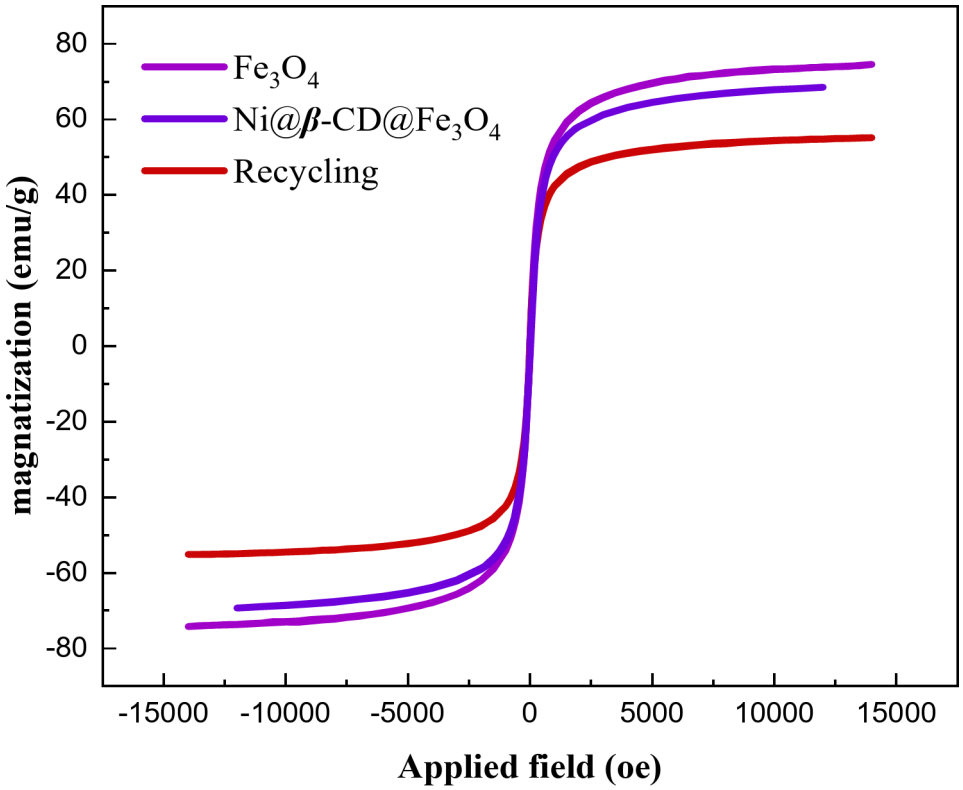

Fig. 6. VSM image of Ni@β-CD@Fe_3O_4 NPs and recycle catalyst after five runs.

the nanocatalyst was transferred to a new flask and employed in the next run. The catalyst was recyclable five successive times with slight decreases in its catalytic activity (Fig. 8).

FT-IR spectrum of the recycled nanocatalyst after five times indicated the conservation of the nanocatalyst (Fig. 9).

Also, the DRS-UV-Vis spectra of the recycle nanocatalyst after five runs indicated a similar pattern to that of the fresh catalyst (Fig. 10).

The VSM of Ni@β-CD@Fe_3O_4 reused the catalyst five times (Fig. 11).

Experimental

Chemicals and instruments

Chemicals were provided by Merck, Across, and Sigma-Aldrich. Reactions were followed by GC on a Varian CP-3800 device. The progress of the nitro reduction reactions was monitored by Analytical TLC (silica gel). Infrared spectra were conducted using utilizing a Bruker Vector 22 spectrometer. The crystallographic structures of the catalyst were characterized by X-ray diffraction (XRD) using a Philips X'Pert Pro apparatus. The FE-SEM mapping and TEM images were captured with Philips CM30 and EOL JEM-2010, respectively. The magnetic feature was measured with a VSM at 25 ℃ from − 15,000 to + 15,000 Oe. TGA was conducted from 30 to 800 °C under a nitrogen flow rate of 20 mL min^{-1} with a NETZSCH STA apparatus. The Varian SpectrAA 110 atomic absorption spectrometer was employed to measure the amount of nickel in the nanocatalyst. DRS-UV-Vis was examined on a Perkin-Elmer Lambda 25 apparatus.

Synthesis of Fe_3O_4 NPs

Fe_3O_4 nanoparticles were made ready in a co-precipitation according to Massart's method by employing $FeCl_3{\cdot}6H_2O$ and $FeCl_2{\cdot}4H_2O$. Fe_3O_4 nanoparticles were synthesized by the reaction of ferrous salts ($FeCl_2{\cdot}4H_2O$ and $FeCl_3{\cdot}6H_2O$ with a molar ratio of 1:2). Usually, $FeCl_3{\cdot}6H_2O$ (0.0216 mmol, 5.838 g) and $FeCl_2{\cdot}4H_2O$ (0.0108 mmol, 2.147 g) was solvated in distilled water (100 mL) under an Ar atmosphere and strong stirring. Next, ammonia (25%, 10 mL) was added up leisurely under an Ar atmosphere, and the resulting combination was stirred at 70 ℃ for 24 h. Adding the base to the Fe^{2+}/Fe^{3+} salt solution led to the construction of nanoparticles that were removed with a magnet, washed several runs by EtOH and distilled H_2O, and dried in an oven overnight to provide magnetic nanoparticles.

The preparation of β-CD@Fe_3O_4

A solution of β-CD (1 g) in deionized H_2O (10 mL) was stirred at 25 ℃ for 15 min, and the mixture was moved to a flask including Fe_3O_4 NPs (500 mg in 10 mL of water) and the mixture sonicated for 15 min. Afterwards, this mixture was dispersed utilizing a mechanical stirrer at 70 °C for 24 h. The mixture was cooled to room

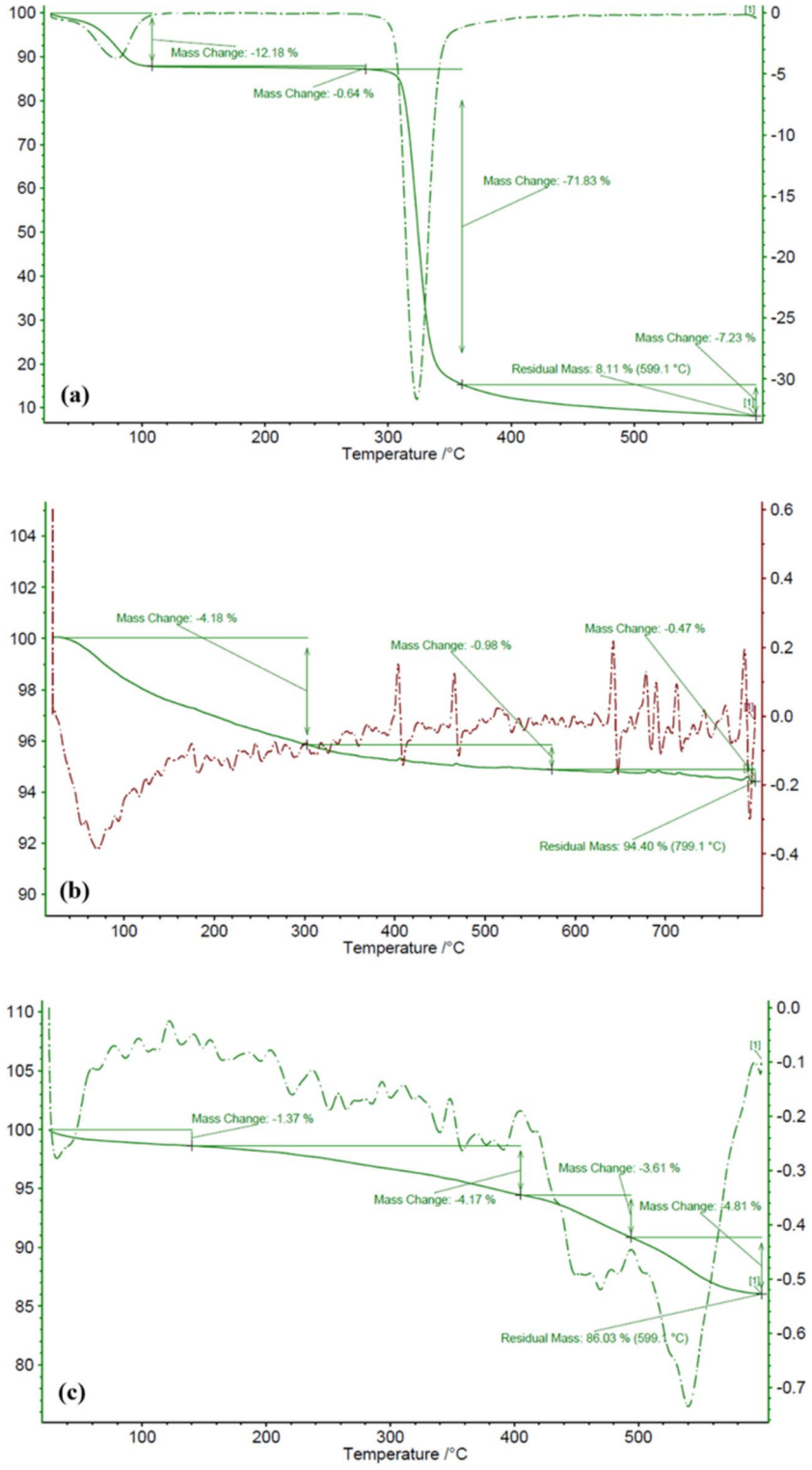

Fig. 7. Thermogravimetric analysis of β-CD (**a**), Fe_3O_4 (**b**), and Ni@β-CD@Fe_3O_4 (**c**).

temperature, and the attained material was centrifuged. The resulting β-CD@Fe_3O_4 was exposed to magnetic separation, and the gained material was rinsed with H_2O/EtOH and dried under vacuum.

The preparation of Ni@β-CD@Fe_3O_4

β-CD@Fe_3O_4 (1 g) was sonicated in H_2O (15 mL) for 15 min. In another flask, nickel acetate (300 mg) was sonicated and dissolved in deionized H_2O (5 mL). The resulting mixture was added to the flask, including β-CD@Fe_3O_4, under an Ar atmosphere, and the mixture was stirred at 70 °C for one night. Next, the resultants

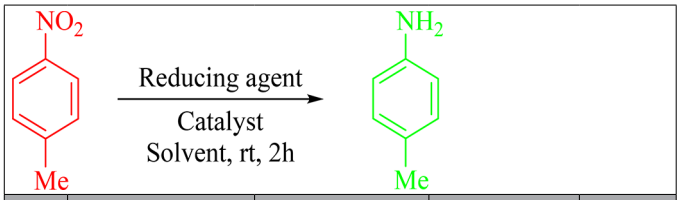

Entry	Ni@β-CD@Fe_3O_4NPs	Reducing agents	Solvent	Yield (%)[a]
1	1.5	$NaBH_4$	DMF	4
2	1.5	$NaBH_4$	THF	5
3	1.5	$NaBH_4$	Toluene	3
4	1.5	$NaBH_4$	DMSO	7
5	1.5	$NaBH_4$	Dichloromethane	6
6	1.5	$NaBH_4$	1,4-Dioxane	8
7	1.5	$NaBH_4$	Ethyl acetate	43
8	1.5	$NaBH_4$	PEG200	18
9	1.5	$NaBH_4$	EtOH	71
10	1.5	$NaBH_4$	Acetone	65
11	1.5	$NaBH_4$	MeOH	35
12	**1.5**	**$NaBH_4$**	**H_2O**	**100**
13	1.5	Isopropyl alcohol	H_2O	48
14	1.5	Ammonium formate	H_2O	N.R
15	1.5	Glycerol	H_2O	Trace
16	1.5	Hydrazine	H_2O	N.R
17	1	$NaBH_4$	H_2O	42

Table 2. The reduction of 4-nitrotoluene under optimization reaction status. Reaction conditions: Nitroarene (0.2 mmol), Ni@β-CD@Fe_3O_4 NPs (15 mg, 1.5 mol% of Ni), solvent (1 mL), and $NaBH_4$ (0.8 mmol) at 25 ℃. [a] GC yields.

were gathered employing a magnet and rinsed with water and EtOH to eliminate the unattached substrates and dry them under a vacuum at 60 °C.

Typical procedure for nitroarenes reduction

Nitroarene (0.2 mmol), $NaBH_4$ (0.8 mmol), catalyst (15 mg, 1.5 mol% nickel), and solvent were added to a 5 mL flask, and the resulting solution was stirred for a proper time at 25 ℃. After completion of the reaction, the reaction mixture was extracted by ethyl acetate and purified using column or plate chromatography.

A plausible mechanism

Based on the previous report[55], a suggested pathway was indicated in Fig. 12. The hydrogenation of the nitroaromatic material has happened through an H^- transfer from sodium borohydride to the $–NO_2$ group to yield a –NO group, which reacted with more H^- to produce the amine derivatives.

Based on previous reports and our experimental results, a possible mechanism for the nitroaromatic reduction using the Ni@β-CD@Fe_3O_4 catalyst is proposed (Fig. 12). The mechanism involves the following steps:

- Hydride transfer: The reduction process begins with the transfer of hydride ions from $NaBH_4$ to the nitro group of the aromatic compound, converting it to a nitroso intermediate.
- Formation of hydroxylamine: Subsequent hydride transfers further reduce the nitroso group to form a hydroxylamine intermediate.
- Final reduction to amine: Additional hydride ions reduce the hydroxylamine to the final amine product.

Mechanistic insights:

Role of Ni@β-CD@Fe_3O_4: The Ni nanoparticles provide active sites for the adsorption and activation of the nitroarene and $NaBH_4$, facilitating efficient hydride transfer.

Stabilization by β-CD: The β-CD grafted onto Fe_3O_4 enhances the dispersion and stability of Ni nanoparticles, ensuring consistent catalytic activity.

This proposed mechanism aligns with the observed high conversion rates and selectivity for amine products, underscoring the effectiveness of Ni@β-CD@Fe_3O_4 as a green and recyclable catalyst for nitroaromatic reductions.

These interpretations comprehensively understand the catalyst's performance and underlying reduction mechanism, contributing to green chemistry and sustainable catalytic processes.

Entry	Nitroaromatic compound	Product	Time (h)	Yield (%)	TON	TOF
1	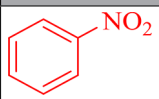	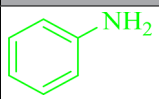	1	99	330	660
2	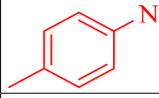	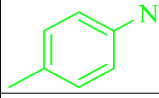	1	98	327	653
3	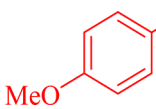	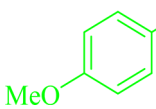	3	97	323	646
4	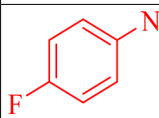	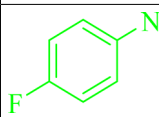	1.5	98	327	653
5	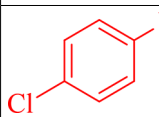	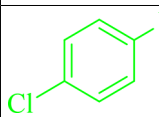	1.5	97	323	646
6	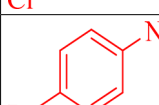	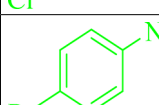	2	85	283	566
7	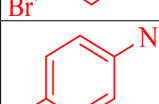	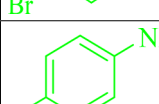	2	84	279	559
8	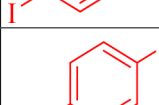	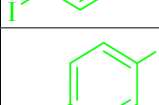	4	98	327	653
9	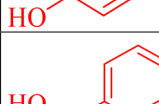	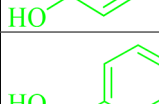	1.5	90	300	600
10	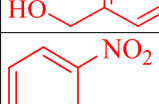	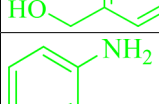	2.5	94	313	626
11	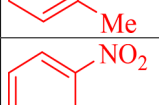	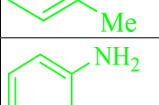	4	89	296	593
12	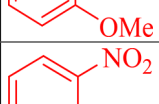	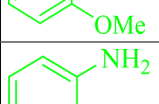	2	92	306	613
13	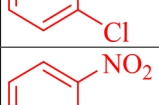	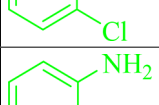	2	94	313	626
14	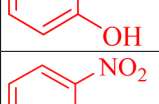	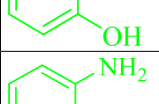	1.5	90	300	600
15	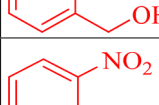	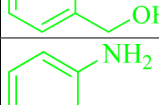	2.5	90	300	600

Continued

Entry	Nitroaromatic compound	Product	Time (h)	Yield (%)	TON	TOF
16	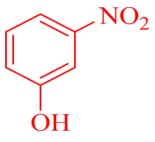	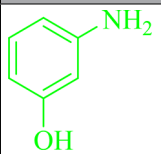	3	91	303	606
17	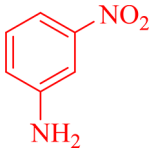	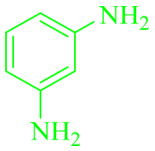	3	92	306	613
18	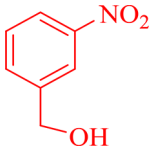	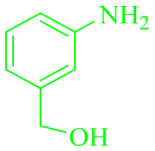	2.5	93	310	620
19	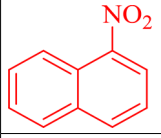	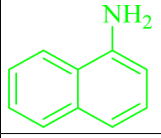	4	83	276	553
20	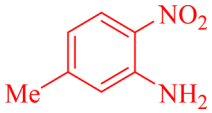	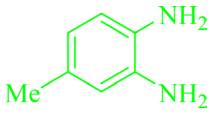	4	88	293	586

Table 3. The reduction of diverse nitro compounds using Ni@β-CD@Fe_3O_4 NPs as a catalyst. Reaction conditions: Nitroarene (0.2 mmol), Ni@β-CD@Fe_3O_4 NPs (15 mg, 1.5 mol%), H_2O (1 mL), and reducing agent (0.8 mmol) at room temperature.

Entry	Catalyst	Temp. (°C)	Time (h)	Solvent	Ni (mol%)	Yield (%)	Ref.
1	Ni/C catalyst	25	5.5–8.5	H_2O/ MeOH	20 mg	92–99	21
2	Ni/$NiFe_2O_4$	70	3	H_2O	70 mg	82.3–90	22
3	Ni/SiC-$B_{0.5}$	90	1	EtOH	50 mg	70.1–95.5	23
4	Ni@N – C catalyst	25	5 min	MeOH	6	20–99	24
5	$NiCl_2.6H_2O$/dppe	100	12	EtOH	2.5	72–97	25
6	Ni@β-CD@Fe_3O_4NPs	25	1–4	H_2O	1.5	83–99	This work

Table 4. A comparison of the results of the present system with the previous reports.

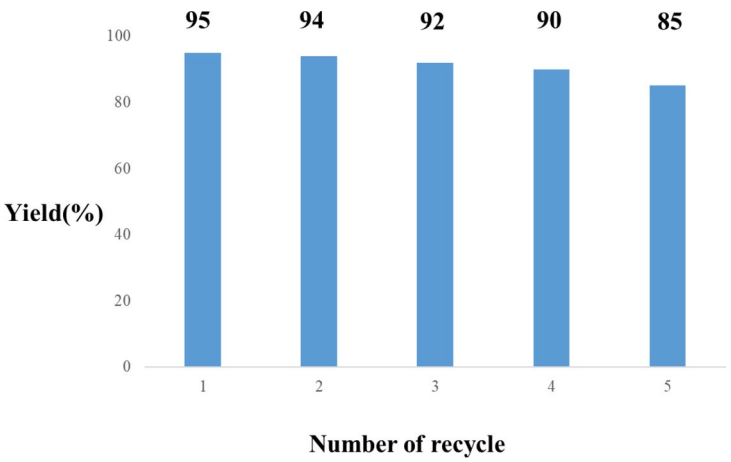

Fig. 8. Recycling Ni@β-CD@Fe_3O_4 NPs catalyst in nitro aromatic reduction.

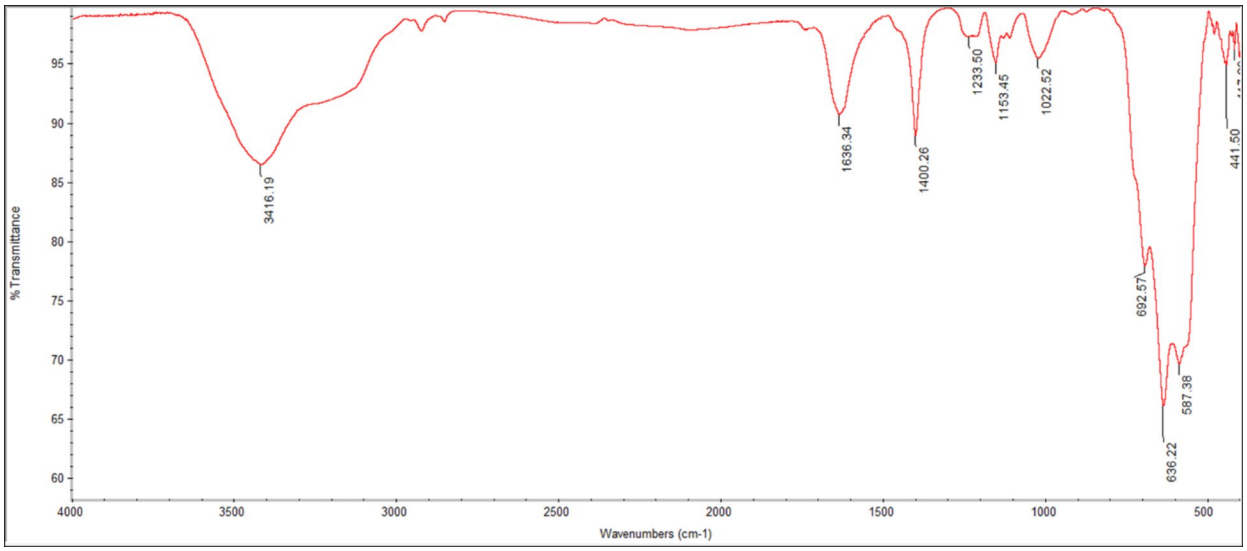

Fig. 9. FT-IR photograph of recycled nanocatalyst five times.

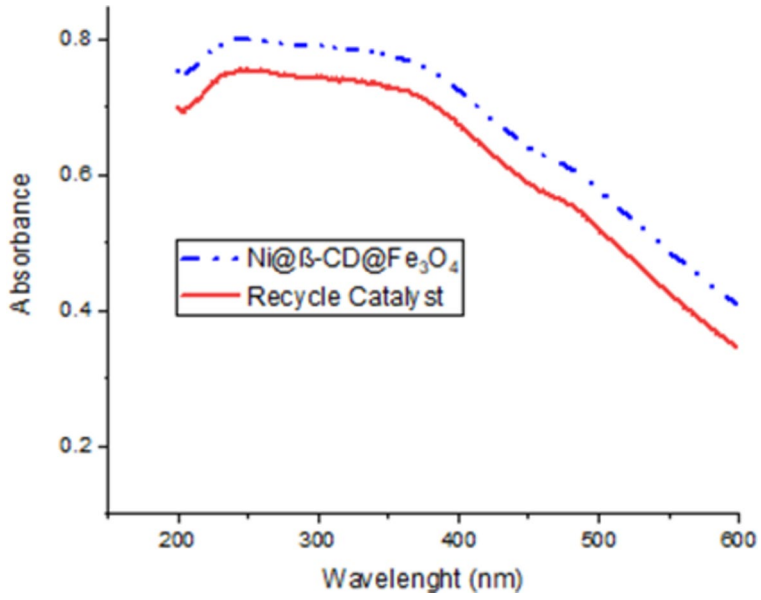

Fig. 10. DRS-UV-Vis spectra of Ni@β-CD@Fe_3O_4 NPs after recyclability test five times.

Conclusion

This study successfully synthesized a novel, highly active, and separable heterogeneous catalyst by immobilizing nickel nanoparticles onto β-CD grafted magnetic Fe_3O_4 nanoparticles (Ni@β-CD@Fe_3O_4). This catalyst demonstrated exceptional catalytic activity and recyclability in reducing nitroaromatic compounds in aqueous media. The incorporation of β-CD provided a biocompatible, green, and non-toxic environment, enhancing the overall sustainability of the catalyst.

Key findings from our research include:

1. High catalytic efficiency: The Ni@β-CD@Fe_3O_4 catalyst effectively reduced various nitroarene derivatives, achieving high conversion rates and selectivities under mild conditions.
2. Recyclability and stability: The catalyst exhibited excellent stability and could be easily separated from the reaction mixture utilizing an external magnetic, allowing for multiple reuse cycles without significant activity loss.
3. Green chemistry principles: The synthesis and application of this catalyst align with green chemistry principles, emphasizing the use of non-toxic materials, energy efficiency, and waste reduction.

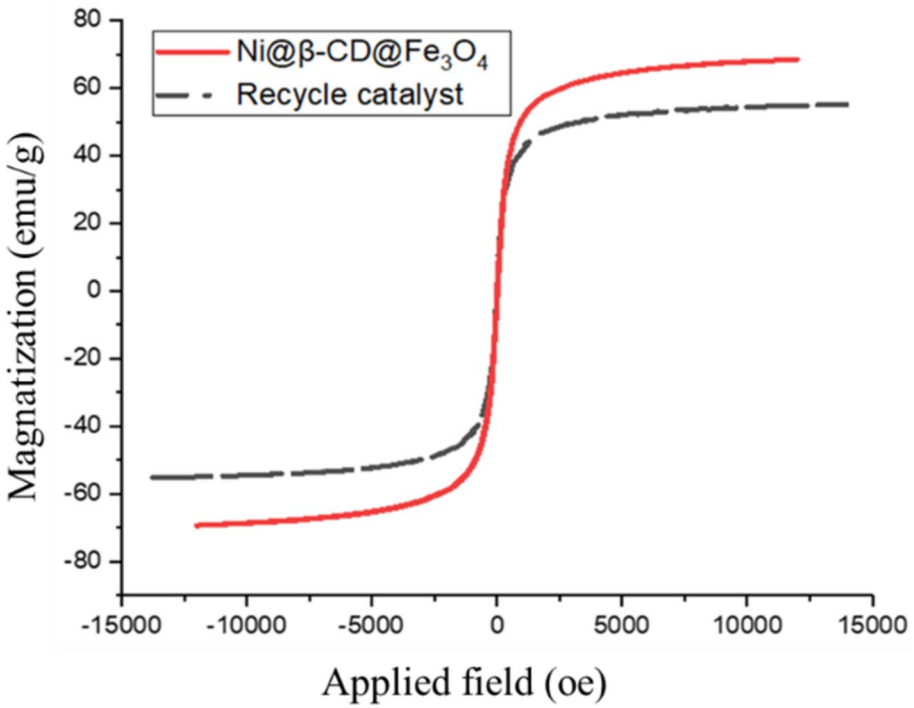

Fig. 11. VSM curves of Ni@β-CD@Fe_3O_4 and reused catalyst five runs.

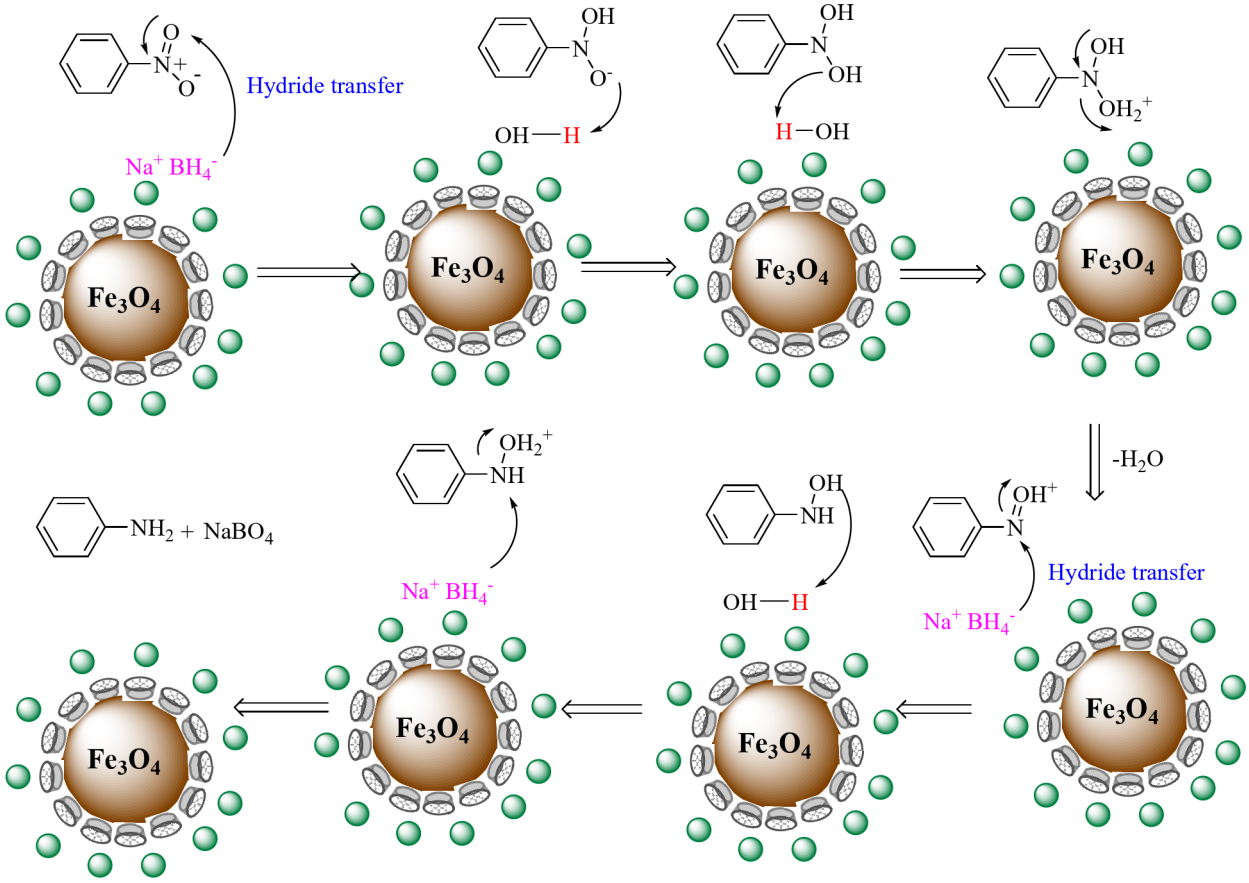

Fig. 12. A suggested mechanism for the hydrogenation of nitrobenzene in the existence of Ni@β-CD@Fe_3O_4.

These results highlight the potential of Ni@β-CD@Fe_3O_4 as a viable alternative to traditional palladium-based catalysts, offering a more sustainable and cost-effective solution for industrial applications involving the reduction of nitroaromatic compounds. Future research will optimize the synthesis process and explore the catalyst's performance in a broader range of chemical reactions. Additionally, scaling up the production and evaluating the economic feasibility of industrial applications will be crucial next steps.

Data availability

All data have been given in the article.

Received: 2 July 2024; Accepted: 12 November 2024
Published online: 18 November 2024

References

1. Sheldon, R. A. Metrics of green chemistry and sustainability: past, present, and future. *ACS Sustainable Chem. Eng.* **6**, 32–48 (2018).
2. Płotka-Wasylka, J. et al. Green chemistry in higher education: state of the art, challenges, and future trends. *ChemSusChem*. **11**, 2845–2858 (2018).
3. Payamifar, S., Behrouzi, L. & Poursattar Marjani, A. The electrochemical coupling reactions of organic halides compound in a valuable and practical manner for CC and C–heteroatom formation: an overview. *Arab. J. Chem.* **17**, 105822 (2024).
4. Goksu, H., Sert, H., Kilbas, B. & Sen, F. Recent advances in the reduction of nitro compounds by heterogeneous catalysts. *Curr. Org. Chem.* **21**, 794–820 (2017).
5. Kovacic, P. & Somanathan, R. Nitroaromatic compounds: environmental toxicity, carcinogenicity, mutagenicity, therapy and mechanism. *J. Appl. Toxicol.* **34**, 810–824 (2014).
6. Orlandi, M., Brenna, D., Harms, R., Jost, S. & Benaglia, M. Recent developments in the reduction of aromatic and aliphatic nitro compounds to amines. *Org. Process. Res. Dev.* **22**, 430–445 (2016).
7. Nishiwaki, N. A walk through recent nitro chemistry advances. *Molecules*. **25**, 3680 (2020).
8. Murahashi, S. I. & Imada, Y. Synthesis and transformations of nitrones for organic synthesis. *Chem. Rev.* **119**, 4684–4716 (2019).
9. Kadam, H. K. & Tilve, S. G. Advancement in methodologies for reduction of nitroarenes. *RSC Adv.* **5**, 83391–83407 (2015).
10. Payamifar, S. & Poursattar Marjani, A. Recent advances in β-cyclodextrin-based catalysts for reducing toxic nitroaromatic: an overview. *Appl. Organomet. Chem.* **37**, e7287 (2023).
11. Béchamp, A. De l'action des protosels de fer sur la nitronaphtaline et la nitrobenzine; nouvelle méthode de formation des bases orgnaiques artificielles de zinin. *Ann. Chim. Phys.* **42**,186 (1854).
12. Formenti, D., Ferretti, F., Scharnagl, F. K. & Beller, M. Reduction of nitro compounds using 3d-non-noble metal catalysts. *Chem. Rev.* **119**, 2611–2680 (2018).
13. Das, T. K. & Das, N. C. Advances on catalytic reduction of 4-nitrophenol by nanostructured materials as benchmark reaction. *Int. Nano Lett.* **12**, 223–242 (2022).
14. Ferretti, F., Ramadan, D. R. & Ragaini, F. Transition metal catalyzed reductive cyclization reactions of nitroarenes and nitroalkenes. *ChemCatChem*. **11**, 4450–4488 (2019).
15. Bibak, S., Poursattar Marjani, A. & Sarreshtehdar Aslaheh, H. MCM-41 supported 2-aminothiophenol/Cu complex as a sustainable nanocatalyst for Suzuki coupling reaction. *Sci. Rep.* **14**, 18070 (2024).
16. Yan, Z. et al. Tandem selective reduction of nitroarenes catalyzed by palladium nanoclusters. *Green. Chem.* **22**, 1301–1307 (2020).
17. Çalışkan, M., Baran, T. & Nasrollahzadeh, M. Facile preparation of nanostructured Pd-Sch-δ-FeOOH particles: a highly effective and easily retrievable catalyst for aryl halide cyanation and p-nitrophenol reduction. *J. Phys. Chem. Solids*. **152**, 109968 (2021).
18. Gan, D. et al. Green synthesis of bimetallic PdAg alloy nanoparticles supported on polydopamine-functionalized kaolin for catalytic reduction of 4-nitrophenol and organic dyes. *Appl. Clay Sci.* **244**, 107091 (2023).
19. Wang, J. et al. Magnetic boron nitride adorned with pd nanoparticles: an efficient catalyst for the reduction of nitroarenes in aqueous media. *Dalton Trans.* **52**, 3567–3574 (2023).
20. Daneshafruz, H., Mohammadi, P., Barani, H. & Sheibani, H. Facile synthesis of magnetic bentonite–chitosan–Pd nanocomposite: as a recoverable nanocatalyst for reduction of Nitroarenes and Suzuki–Miyaura reaction. *J. Inorg. Organomet. Polym. Mater.* **33**, 1052–1065 (2023).
21. Tang, Q. et al. Biomass-derived carbon-supported Ni catalyst: an effective heterogeneous non-noble metal catalyst for the hydrogenation of nitro compounds. *React. Chem. Eng.* **5**, 58–65 (2020).
22. More, G. S., Kharb, S., Gill, P. & Srivastava, R. Enhancing nitroaromatics reduction through synergistic participation of Ni NPs and nickel ferrite/C nanocomposite: a path towards greener industrial viability. *Appl. Catal. A: Gen.* **681**, 119785 (2024).
23. Zhao, J. X. Enhanced catalytic performance of B-doped SiC supported Ni catalysts for the hydrogenation of nitroarenes. *Appl. Catal. A: Gen.* **678**, 119726 (2024).
24. Cao, L. et al. Chemoselective nitro reduction using nitrogen-doped carbon-encapsulated ni catalyst and Y-Type packed bed column for continuous flow reaction. *Adv. Synth. Catal.* **365**, 2230–2239 (2023).
25. Dewangan, C., Kumawat, S., Bhatt, T. & Natte, K. Homogenous nickel-catalyzed chemoselective transfer hydrogenation of functionalized nitroarenes with ammonia–borane. *ChemComm*. **59**, 14709–14712 (2023).
26. Keyhaniyan, M., Shiri, A., Eshghi, H. & Khojastehnezhad, A. Synthesis, characterization and first application of covalently immobilized nickel-porphyrin on graphene oxide for Suzuki cross-coupling reaction. *New. J. Chem.* **42**, 19433–19441 (2018).
27. Khojastehnezhad, A. et al. Size-dependent catalytic activity of palladium nanoparticles decorated on core–shell magnetic microporous organic networks. *ACS Appl. Nano Mater.* **6**, 17706–17717 (2023).
28. Arefi, E., Khojastehnezhad, A. & Shiri, A. A magnetic copper organic framework material as an efficient and recyclable catalyst for the synthesis of 1,2,3-triazole derivatives. *Sci. Rep.* **11**, 20514 (2021).
29. Keyhaniyan, M., Khojastehnezhad, A., Eshghi, H. & Shiri, A. Magnetic covalently immobilized nickel complex: a new and efficient method for the Suzuki cross-coupling reaction. *Appl. Organomet. Chem.* **35**, e6158 (2021).
30. Ghadamyari, Z., Khojastehnezhad, A., Seyedi, S. M. & Shiri, A. Co(II)-porphyrin immobilized on graphene oxide: an efficient catalyst for the Beckmann rearrangement. *ChemistrySelect*. **4**, 10920–10927 (2019).
31. Khojastehnezhad, A., Bakavoli, M., Javid, A., Khakzad Siuki, M. M. & Shahidzadeh, M. Synthesis, characterization, and investigation of catalytic activity of copper(II) porphyrin graphene oxide for azide–alkyne cycloaddition. *Res. Chem. Intermed.* **45**, 4473–4485 (2019).
32. Khojastehnezhad, A., Moeinpou, F. & Vafaei, M. Molybdenum oxide supported on silica (MoO_3/SiO_2): an efficient and reusable catalyst for the synthesis of 1,8-dioxodecahydroacridines under solvent-free conditions. *J. Mex Chem. Soc.* **59**, 29–35 (2015).
33. Ghadamyari, Z., Khojastehnezhad, A., Seyedi, S. M., Taghavi, F. & Shiri, A. Graphene oxide functionalized Zn(II) salen complex: an efficient and new route for the synthesis of 1,2,3-triazole derivatives. *ChemistrySelect*. **5**, 10233–10242 (2020).
34. Szejtli, J. Introduction and general overview of cyclodextrin chemistry. *Chem. Rev.* **98**, 1743–1754 (1998).

35. Payamifar, S. & Poursattar Marjani, A. The recent development of β-cyclodextrin-based catalysts system in click reactions: a review. *Appl. Organomet. Chem.* **38**, e7365 (2024).
36. Crini, G. A history of cyclodextrins. *Chem. Rev.* **114**, 10940–10975 (2014).
37. Sarreshtehdar Aslaheh, H. & Payamifar, S. & Poursattar Marjani, A. A review of the use of the nickel catalyst in azide-alkyne cycloaddition reactions. *Appl. Organomet. Chem*. e7692 (2024).
38. Seggio, M. et al. Visible light-activatable cyclodextrin-conjugates for the efficient delivery of nitric oxide with fluorescent reporter and their inclusion complexes with betaxolol. *New. J. Chem.* **45**, 8449–8455 (2021).
39. Caccamo, D. et al. Intracellular fate and impact on gene expression of doxorubicin/cyclodextrin-graphene nanomaterials at sub-toxic concentration. *Int. J. Mol. Sci.* **21**, 4891 (2020).
40. Pennisi, R. et al. Cancer-related intracellular signalling pathways activated by DOXorubicin/cyclodextrin-graphene-based nanomaterials. *Biomol.* **12**, 63 (2022).
41. Jędrzak, A., Kuznowicz, M. & Jesionowski, T. Mobile-assisted diagnostic biosensor for point-of-care glucose detection in real human samples with rapid response and long-live stability. *J. Appl. Electrochem.* **54**, 163–174 (2024).
42. Payamifar, S., Foroozandeh, A., Pourmadadi, M. & Abdouss, M. Cyclodextrin nanocarriers in coordination chemistry: enhancing encapsulation and targeted delivery of 5-Fluorouracil for cancer treatment. *Results Chem.* **12**, 101878 (2024).
43. Kuznowicz, M., Jędrzak, A. & Jesionowski, T. Nature-inspired biomolecular corona based on poly (caffeic acid) as a low potential and time-stable glucose biosensor. *Molecules*. **28**, 7281 (2023).
44. Payamifar, S. & Poursattar Marjani A. A new β-cyclodextrin-based nickel as green and water-soluble supramolecular catalysts for aqueous Suzuki reaction. *Sci. Rep.* **13**, 21279 (2023).
45. Payamifar, S., Kazemi, F. & Kaboudin, B. Nickel/β-CD-catalyzed Suzuki–Miyaura cross-coupling of aryl boronic acids with aryl halides in water. *Appl. Organomet. Chem.* **35**, e6378 (2021).
46. Payamifar, S., Abdouss, M. & Poursattar Marjani, A. The recent development of β-cyclodextrin-based catalysts system in Suzuki coupling reactions. *Appl. Organomet. Chem.* **38**, e7458 (2024).
47. Payamifar, S., Abdouss, M. & Poursattar Marjani, A. Recent advances in β-cyclodextrin-based catalyst systems for the synthesis of heterocyclic compounds via multicomponent reactions (MCRs). *Arab. J. Chem.* **17**, 105967 (2024).
48. Roy, S. Photocatalytic materials for reduction of nitroarenes and nitrates. *J. Phys. Chem. C.* **124**, 28345–28358 (2020).
49. Wu, J. & Darcel, C. Recent developments in manganese, iron and cobalt homogeneous catalyzed synthesis of primary amines via reduction of nitroarenes, nitriles and carboxamides. *Adv. Synth. Catal.* **365**, 948–964 (2023).
50. Orlandi, M., Brenna, D., Harms, R., Jost, S. & Benaglia, M. Recent developments in the reduction of aromatic and aliphatic nitro compounds to amines. *Process. Res. Dev.* **22**, 430–445 (2016).
51. Aditya, T., Pal, A. & Pal, T. Nitroarene reduction: a trusted model reaction to test nanoparticle catalysts. *ChemComm*. **51**, 9410–9431 (2015).
52. Hasan, K., Shehadi, I. A., Joseph, R. G., Patole, S. P. & Elgamouz, A. β-Cyclodextrin-functionalized Fe_3O_4-supported Pd-nanocatalyst for the reduction of nitroarenes in water at mild conditions. *ACS Omega*. **8**, 23901–23912 (2023).
53. Massart, R. Preparation of aqueous magnetic liquids in alkaline and acidic media. *IEEE Trans. Magn.* **17**, 1247–1248 (1981).
54. Kaboudin, B., Mostafalu, R. & Yokomatsu, T. Fe_3O_4 nanoparticle-supported Cu(II)-β-cyclodextrin complex as a magnetically recoverable and reusable catalyst for the synthesis of symmetrical biaryls and 1,2,3-triazoles from aryl boronic acids. *Green. Chem.* **15**, 2266–2274 (2013).
55. El-Hout, S. et al. A green chemical route for synthesis of graphene supported palladium nanoparticles: a highly active and recyclable catalyst for reduction of nitrobenzene. *Appl. Catal. A*. **503**, 176–185 (2015).

Acknowledgements

The authors would like to acknowledge the support from the Research Council of Urmia University and Amirkabir University of Technology.

Author contributions

Sara Payamifar: Data curation, investigation, methodology, writing – original draft. Amin Foroozandeh: Writing – original draft. Majid Abdouss: Supervision. Ahmad Poursattar Marjani: Supervision, writing - review and edition.

Declarations

Competing interests

The authors declare no competing interests.

Additional information

Correspondence and requests for materials should be addressed to A.P.M.

Reprints and permissions information is available at www.nature.com/reprints.

Publisher's note Springer Nature remains neutral with regard to jurisdictional claims in published maps and institutional affiliations.